Reaction and Ignition Delay Times in the Oxidation of Propane

B. F. MYERS* AND E. R. BARTLE†
General Dynamics/Convair, San Diego, Calif.

Empirical correlations between "reaction" and "ignition delay" times and the pressure, temperature, and composition have been obtained for propane-oxygen-argon mixtures. Experiments were conducted by shock heating these mixtures to initial pressures and temperatures between 0.5 and 5.5 atm and 1000° and 1600°K for equivalence ratios and dilutions in the ranges 0.1 to 1.5 and 80 to 99% Ar, respectively. The radiation emitted behind incident shock waves was monitored as a function of time simultaneously in 9 spectral channels in the wavelength range 0.23–5.1μ and the refractive index gradient-time profile was recorded using a laser-schlieren technique. Reaction times were determined from 1) the cessation of CO_2 formation, 2) the termination of OH emission, and 3) termination of the refractive index gradient signal; the ignition delay times were determined from 1) an initial rise in OH emission, 2) a second rise in OH emission, and 3) the initial rise in CO_2 emission. The ratio of the reaction to the ignition delay time was found to be significantly greater than one and in the case of most interest to SCRAMJET applications this ratio was as large as 50. The restrictions on the utility of the empirical correlations for reaction and ignition delay times resulting from the occurrence of detonations and the introduction of systematic error by shock wave attenuation, boundary-layer growth, flow instabilities, and the difficulty of transforming observations from laboratory to particle coordinates are discussed.

Nomenclature

A_i = area under refractive index gradient extremum, arbitrary units
$C_0(\tau)$ = a constant for each reaction and ignition delay parameter, mole-sec-cm^{-3}-atm$^{-5/8}$
$E_a(\tau)$ = a constant for each reaction and ignition delay parameter, cal-mole^{-1}
$g(X_R,\phi)$ = a function which accounts for minor dependencies of α on X_R and ϕ
HTG = heat-transfer gage
l_m = limiting separation between shock front and contact surface, cm
n,n' = exponent of ϕ in the function $g(X_R,\phi)$
P = pressure, atm
R = gas constant, cal-mole^{-1}-°K^{-1}
R' = gas constant, atm-cm^3-mole^{-1}-°K^{-1}
RIG = refractive index gradient
T = temperature, °K
X_R = mole fraction of reactants, $X_R = X_{C_3H_8} + X_{O_2}$
α = a function of ϕ, X_R, P, τ, and T, mole-sec-cm^{-3}-atm$^{-5/8}$
λ_c = center wavelength of spectral interval, μ
$\Delta\lambda$ = bandwidth of spectral interval, μ
μ = wavelength, μ
ν = wavenumber, cm^{-1}
ρ = density, g-cm^{-3}
ρ_{fl} = density ratio across the shock front
$\Delta\rho$ = change in density, g-cm^{-3}
$\tau(y)$ = characteristic time or reaction time for observable y, sec (unless otherwise indicated)
$\tau_I(y),\tau'_I(y)$ = ignition delay time for observable y, sec (unless otherwise indicated)
$\bar{\tau}$ = reaction time computed using the average values of C_0 and E_a, sec
ϕ = equivalence ratio, $\phi \equiv (F/O_2)(F/O_2)_s^{-1}$ where F is the fuel and O_2 the oxygen concentration, and s refers to the stoichiometric ratio

Subscripts

e = final equilibrium
f = frozen state immediately behind the incident shock front before chemical reaction begins but assuming equilibration of internal degrees of freedom.
i = interval in density values
L = laboratory
p = particle
l = preshock conditions

Presented as Paper 68-633 at the AIAA 4th Propulsion Joint Specialist Conference, Cleveland, Ohio, June 10–14, 1968; submitted June 10, 1968; revision received February 14, 1969. This research was supported by the Air Force Aero Propulsion Laboratory, Wright-Patterson Air Force Base, under Contract F33615-67-C-1382. The authors thank E. A. Meckstroth and M. R. Schoonover for assistance with the experiments and numerical calculations.

* Staff Scientist, Space Science Laboratory.
† Staff Scientist, Space Science Laboratory. Member AIAA.

Introduction

THE reaction time is a primary datum in the design of the combustor for supersonic combustion applications.[1–4] This reaction time can be calculated provided a set of elementary reactions and corresponding rate coefficients accurately representing the detailed chemical processes are known. For hydrogen oxidation[3] and propane oxidation,[5] reaction times have been calculated; in the former case, a correlation was established between the reaction time and the temperature and pressure. For propane oxidation, the calculation of reaction time was found to be a difficult task[5] with the data on reactions and rate coefficients presently available. In the present experiments, an attempt has been made to measure the reaction time for the oxidation of propane and to establish an empirical correlation between the temperature, pressure, and composition existing behind an incident shock wave before chemical reaction begins and the reaction time, as well as the ignition delay time, which is simultaneously measured.

The results of the present studies are in qualitative agreement with the calculations of reaction and ignition delay times in propane oxidation[5] as well as with earlier measurements[6] of reaction times in other fuel systems; however, the calculated reaction times are generally smaller than the times measured in this study. By contrast, the ignition delay times

previously measured[7] for propane oxidation are in excellent agreement with data presented here.

Experimental

The experiments were conducted with a 3-in.-i.d., stainless-steel shock tube. This shock tube and associated equipment have been described in detail elsewhere.[8,9] In the following paragraphs, brief descriptions are given of 1) the instrumentation used to measure simultaneously the radiation emitted in nine spectral intervals extending from about 0.23 to 5.1μ, and the laser-schlieren system used to measure the refractive index gradient, 2) the materials, and 3) the experimental procedure.

Apparatus

The spectral intervals in which the radiation emitted by the shock heated gases was monitored are given in Table 1. For each spectral interval, the center wavelength, bandpass, and the species which radiates in the interval, excepting channels 3 and 8, are listed.

The emission from CO and CO_2 was recorded as previously described in detail[8] by monitoring spectral portions of the CO and CO_2-ν_3 fundamental bands. In addition, for some of the experiments, the emission from H_2O was recorded by monitoring spectral portions of the H_2O-($\nu_2 + \nu_3$) and H_2O-ν_3 bands. This was accomplished by using the combination of an InSb detector and narrow bandpass, interference filter ($\Delta\lambda \approx 0.1\mu$). Two filters were used with center wavelengths of 1.95 and 2.5μ, respectively. For the spectral regions spanned by these filters, emission from mixtures containing H_2O and CO_2 at high temperature results only from H_2O over the range of conditions employed in the present experiments.[10]

In the wavelength interval between 0.25 and 0.80μ, the optical and detection system employed, which has been described in detail elsewhere,[11] consisted of an $f/12$ Hilger Medium Quartz Spectrograph which could receive radiation from the shock-heated gases. In the image plane of the spectrograph, 6 slits were placed and calibrated as previously described.[11,12] The radiation passing through these slits was detected by the six photomultipliers.

The response time of all detectors was less than 1 μsec and the optical system did not allow scattered light to reach the detectors. The entire optical system was enclosed in a light-tight box which was purged with dry nitrogen prior to and during an experiment.

The refractive index gradient (RIG) of the shock-heated gases was measured as a function of time with a narrow beam, laser-schlieren technique devised by Kiefer and Lutz.[13] Light from a laser (Spectra Physics Model 122, helium-neon gas laser; $\lambda = 0.6328\mu$) passed perpendicularly through the shock tube and was deflected by a change in the refractive index of the gas. The effective diameter of the laser beam was 0.8 mm in the center of the shock tube and 12.0 mm at a detection station located 7.2 m from the shock tube axis. The laser beam passed through the shock tube at an observation station located 57.15 mm upstream of the observation station used for the spectroscopic measurements. The complete system was estimated to have a rise time of less than 0.1 μsec.

The laser-schlieren system of these experiments differed in two respects from the system of Kiefer and Lutz.[13] First, at the detector station, the conventional knife edge of a schlieren system was replaced with a beam splitter consisting of two right angle prisms butted together. The split beams were focused by lenses onto photodiodes (Edgerton, Germeshausen, and Grier Inc. Model S-100); the difference of the output signals was recorded. Second, the laser beam was not focused or reduced in diameter before reaching the detector station. With this arrangement, the sharp signal spike associated with the large density gradients in the beam path during shock front passage was preceded by a signal deflection of opposite sign. The peak intensity of the latter signal was approximately proportional to the initial pressure of the test gas for a constant Mach number. It could be eliminated by focusing the incident laser beam in the center of the shock tube and recollimating the laser beam on the exit side, although this was not done for the present experiments. Reflection of the laser beam by the shock front before extensive refraction of the beam may contribute to the formation of the initial signal; however, the true mechanism is not known at present. The use of the RIG as outlined below does not depend on the occurrence of this initial signal.

Table 1 Spectroscopic channels utilized

Channel	λ_c,μ	$\Delta\lambda,\mu$	Pertinent radiator
1	4.25	0.043	CO_2-γ_3
2	5.07	0.130	CO
3	0.2300	0.0062	...
4	0.3095	0.0030	OH
5	0.3930	0.0100	CN
6	0.4300	0.0100	CH
7	0.5200	0.0100	C_2
8	0.7253	0.0206	...
9	2.50	0.040	H_2O-ν_3
10	1.95	0.040	H_2O-($\nu_3 + \nu_2$)

Materials

The principal impurities of the test gases and the purity levels as given by the manufacturer are listed in Ref. 14. Test gas mixtures were prepared in a gas handling facility which has been described in detail elsewhere.[9] The concentrations of the gas mixture constituents were determined by partial pressure measurements.

Procedure

The experiments were conducted by shock heating test gas mixtures of propane, oxygen, and argon to temperatures between 1000° and 1600°K and pressures between 0.5 and 5.5 atm. The emission intensity in spectral channels 1–8 of Table 1 and the RIG were recorded as a function of time simultaneously. In a selected number of experiments, emission signals in channel 9 or 10 were recorded in place of those in channel 2. Contributions to the recorded emission intensities from the test gas constituents and accompanying impurities were investigated by shock heating Ar, 20% O_2 + 80% Ar, and 5% C_3H_8 + 95% Ar to a temperature of about 2500°K and a pressure of about 2 atm. No signals were detected in channels 1–8 of Table 1 for the mixtures. When channel 9 or 10 was employed, the emission from shock-heated mixtures of 5% C_3H_8 + 95% Ar indicated the presence of a small water impurity ($\lesssim$0.1%) in the propane. This signal was only slightly attenuated when the propane was first frozen at dry ice temperature and pumped on. However, the influence of this impurity on the reaction parameters measured (as described below) is considered negligible.

The initial thermodynamic state and the equilibrium thermodynamic state for each test gas mixture behind the incident shock wave were calculated using one-dimensional normal shock theory. For the initial state calculations, equilibration of the internal degrees of freedom and no chemical reaction were assumed. For the equilibrium calculations, the species included were C_3H_8, O_2, O, CO, CO_2, OH, H_2O, H_2O_2, H, H_2, and CH_2O. The inclusion of additional species, i.e., C_nH_m, where $1 \leq n \leq 4$ and $1 \leq m \leq 10$, had a negligible effect on the composition and thermodynamic state at equilibrium. The calculations were performed on an IBM 360 computer using the Los Alamos GMX-7 shock parameter code.‡

‡ Received by this laboratory through the courtesy of G. L. Schott, Los Alamos Scientific Laboratory, University of California, Los Alamos, N. Mex.

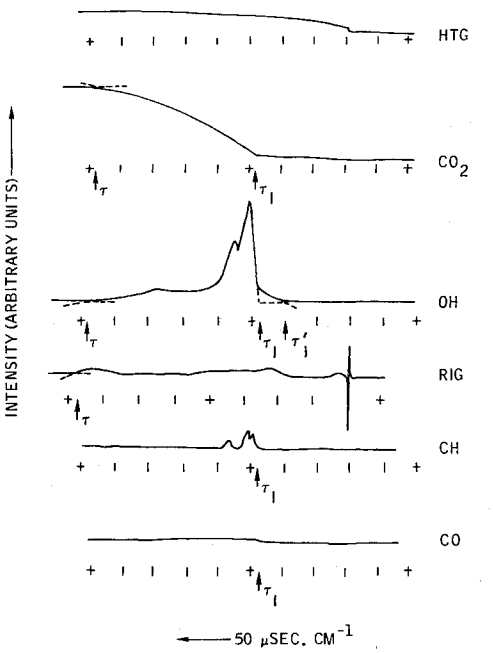

Fig. 1 Observables and characteristic times. Run 1322: T_f = 1321°K, P_f = 1.32 atm, T_e = 1381°K, P_e = 1.28 atm, $C_3H_8 + O_2 + Ar$, ϕ = 0.2, 95% Ar.

Results

Oxidation of Propane

Examples of the experimental results obtained by shock heating mixtures of propane-oxygen-argon are shown by the oscillogram tracings of Figs. 1 and 2 for runs 1322 and 1487, respectively. For Fig. 1, in the order from top to bottom, the tracings show the time histories of 1) the response of a heat-transfer gage (HTG) to shock front arrival at the observation station as indicated by the sudden rise in this trace, 2) CO_2 emission, 3) OH emission, 4) the refractive index gradient, 5) the CH emission, and 6) CO emission. For Fig. 2, the H_2O emission trace has been added and those for CH and CO deleted. (The time scales for the CO and/or RIG traces as shown in Figs. 1 and 2 are slightly different from the other traces.) Emission was not detected in channels 3, 5, 7, and 8. To characterize the reaction and ignition delay time for propane oxidation, 6 distinguishable features were selected from

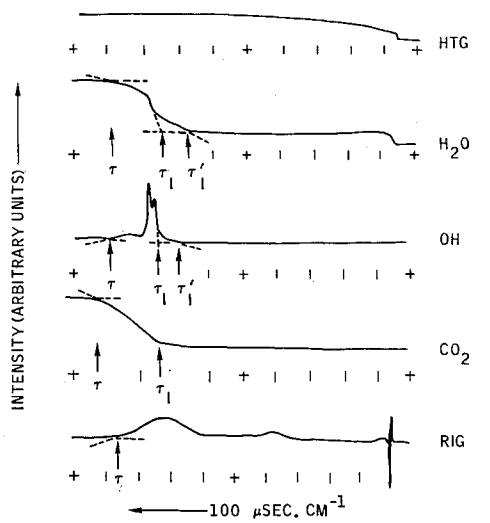

Fig. 2 Observables and characteristic times. Run 1487: T_f = 1301°K, P_f = 1.07 atm, T_e = 1353°K, P_e = 1.04 atm, $C_3H_8 + O_2 + Ar$, ϕ = 1.0, 99% Ar.

the oscillograms for the experiments represented by Figs. 1 and 2 which were also present on the oscillograms of all the experiments. The reaction time τ was determined from three features: 1) the cessation of CO_2 formation as indicated by plateau in the CO_2 emission-time traces, 2) the termination of OH emission, and 3) the termination of the final refractive index gradient extremum. Also, in selected experiments for which H_2O emission was recorded, a reaction time was based on the cessation of H_2O formation. In all cases, the reaction time was evaluated by the extrapolation procedures indicated in Figs. 1 and 2. The ignition delay time τ'_I or τ_I was also determined from three features: 1) the initial rise in OH emission, 2) the second rise in OH emission, and 3) the initial rise in CO_2 emission. Again, in selected experiments where H_2O emission was recorded, the initial and second rise in H_2O emission were the bases for ignition delay times. In all cases, the ignition delay time was evaluated by an extrapolation of portions of the traces to the zero intensity axes as indicated in Figs. 1 and 2. These definitions of reaction time and ignition delay time do not require a knowledge of the relationship between emission and concentration for any of the emitting species or of the relationship between the refractive index gradient and the density and specific refractivity.

The temperature dependence of the selected parameters as well as the relation between them is illustrated in Fig. 3 for the set of experiments with 95% Ar diluent and ϕ = 0.2. The characteristic times τ computed as described below are plotted vs T_f^{-1}. (The lines drawn through the data points are visual estimates and are included to clarify the graphical presentation.) This figure clearly demonstrates that two distinct temperature regions exist for the parameters. The temperature dependence is different above and below about 1300° and 1250°K for the reaction time and ignition delay time, respectively. In addition, the figure also shows that 1) the three reaction times $\tau(CO_2)$, τ(OH), and τ(RIG) as defined previously are practically the same over the experimental temperature range, 2) the ignition delay times τ_I(OH) and $\tau_I(CO_2)$ corresponding to the second rise in OH emission and the onset of CO_2 emission are identical over the entire temperature range,

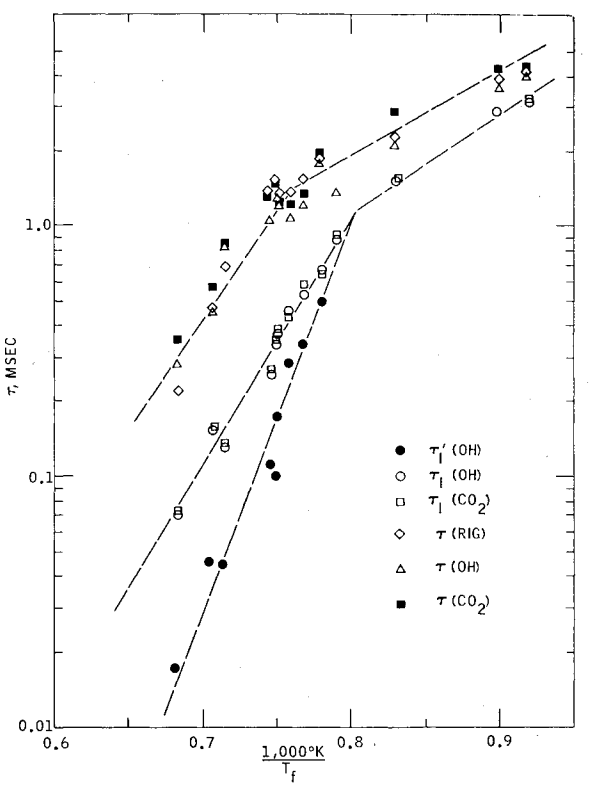

Fig. 3 Reaction and ignition delay times. $C_3H_8 + O_2 + Ar$, $P \approx 1$ atm, ϕ = 0.2, 95% Ar.

and 3) the initial rise in OH emission has a different temperature dependence than the second rise in OH emission above 1250°K. Below 1250°K, the OH emission trace shows only the second rise (i.e., a rise with a slope characteristic of the second rise in OH emission of Fig. 1 or 2). By contrast, there are no qualitative differences after τ_I(OH) in the OH emission traces at temperatures above or below 1250°K except as noted below.[15] In experiments for which the H_2O emission was monitored, the parameters $\tau(H_2O)$, $\tau_I(H_2O)$, and $\tau'_I(H_2O)$ were found to have the same values and therefore temperature dependencies within experimental error as the corresponding parameters for the other observables.

The time profiles of the observables recorded in the propane oxidation experiments show features in addition to those selected for use in characterizing the reaction and ignition delay times. Some of these additional features are illustrated in Figs. 1 and 2. The OH emission profile consists of an initial rise and second rise, already considered, two sharp maxima followed by a broad maximum. This structure of the OH emission profile was observed generally for the propane oxidation experiments, except for the initial rise which was not detected below 1250°K and for experiments in which severe flow instabilities developed (see below); the relative magnitudes of the sharp maxima were observed to change for different experiments (as illustrated by comparing Figs. 1 and 2) and the initial rise in OH emission exhibited a maximum in some of the experiments at higher temperature. When the CH emission trace was intense, the structure was similar to that observed for OH emission, but the CH emission was generally too weak to be used in the data reduction. The weak emission intensity also was found for CO. The RIG traces had a rich but variable structure of extrema which has not been adequately examined in the present study.

The additional, structural features described previously are best illustrated by the data obtained with the mixture having $\phi = 0.2$ and 95% Ar. For these experiments, the following time coincidences were noted: 1) the onset for the initial rise of OH and CH, 2) the onset for the initial rise of CO and CO_2 (see, however, Ref. 16), the onset for the second rise in OH and CH, and the location of a RIG extremum, and 3) the two sharp maxima in OH and CH emission traces and two RIG extrema. In addition, a RIG extremum generally preceded the onset of any detectable emission. In the time coincidences, the OH emission correlates very well with the RIG extrema and if the latter are associated with the heat release process then OH is also. This is in contrast to the H_2-O_2 system, where the rise in OH radical concentration generally precedes the heat release. Above 1250°K, the temperature dependence was found to be the same for 1) the onset for the rise in CO_2, the onset for the second rise in OH, and a RIG extremum, 2) the first of the sharp maxima in OH emission and a RIG extremum, and 3) the second of the sharp maxima in OH emission and a RIG extremum. Furthermore, the temperature dependence of parameter groups 1, 2, and 3 was different. All the time coincidences discussed here, while not generally observable, do indicate that correlations exist other than those used in this study.

Fluid Dynamic Instabilities

The conditions under which experiments with propane-oxygen mixtures could be satisfactorily conducted were limited by the occurrence of detonations and of fluid dynamic instabilities observed in nondetonating systems. The occurrence of a detonation was identified by an increased velocity of shock wave propagation, by large emission signals in all spectral channels with no evidence for an ignition delay, and by a characteristic RIG profile which exhibited large positive and negative signal excursions.[14]

For nondetonating mixtures, flow instabilities were indicated by 1) oscillations in the CO_2 emission, OH emission, and RIG traces and 2) by a double peak in the RIG extremum corresponding to the shock front. The number and magnitude of the oscillations increased with increasing ϕ (up to $\phi \approx 1$), P, or T and with decreasing diluent concentration. An example of relatively severe oscillations is shown in Fig. 4a for a propane-oxygen-argon mixture. In the order from the top to the bottom of the figure, the tracings show the time history of 1) the response of a heat-transfer gage to shock front arrival at the observation station, 2) the CO_2 emission, 3) the OH emission, and 4) the RIG. The double peak observed in the shock front RIG extremum is shown in Fig. 4b for a propane-oxygen-argon mixture; the tracings show the time histories of 1) the time derivative of the heat-transfer gage signal and 2) the RIG. The time resolution for most experiments was relatively small and then the maxima were not separated although a broadening of the shock front RIG extremum was evident. The best single indicator for flow instabilities for the present experiments between 1000° and 1600°K was the CO_2 emission; at small values of ϕ, P, T, and large diluent concentrations the OH emission and RIG signals became weak whereas the CO_2 emission remained strong as a result of the increased emissivity of CO_2 at the lower temperatures for the spectral interval employed (see Table 1).

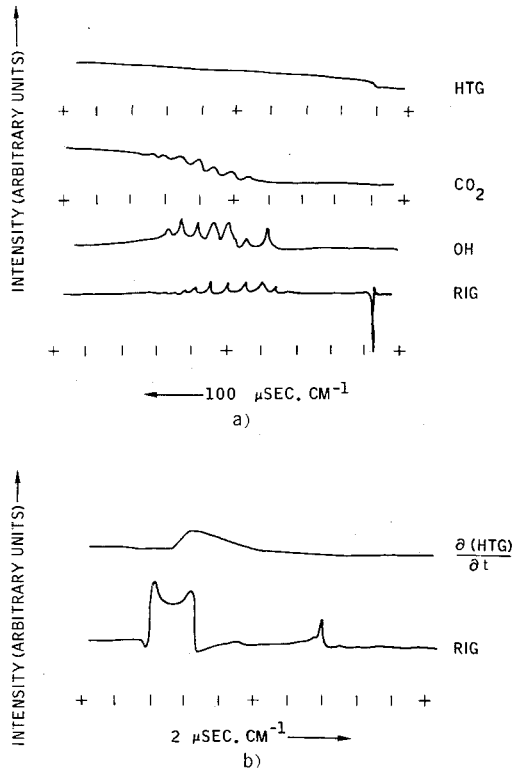

Fig. 4 Influence of flow instabilities. a) Run 1351: T_f = 1204°K, P_f = 0.56 atm, T_e = 1318°K, P_e = 0.52 atm, $C_3H_8 + O_2 + Ar$, ϕ = 0.1, 80% Ar; b) Run 1302: T_f = 1250°K, P_f = 1.01 atm, $C_3H_8 + O_2 + Ar$, ϕ = 1.0, 95% Ar.

By using the experimental indicators described previously, instabilities were detected in 40% of the experiments; the effect of these instabilities on the empirical correlations developed in this study is considered below (see Summary and Discussion).

Correlation of Reaction and Ignition Delay Times

Correlations for the propane oxidation data have been obtained in terms of the six reaction parameters defined previously. Examples of the correlations are shown in Figs. 5 and 6 for the two parameters τ(OH) and $\tau_I(CO_2)$, respectively. The correlation function is αg where

$$\alpha = (5\phi)^{1/2} X_R P_f^{3/8} \tau / [R' T_f (5 + \phi)] \qquad (1)$$

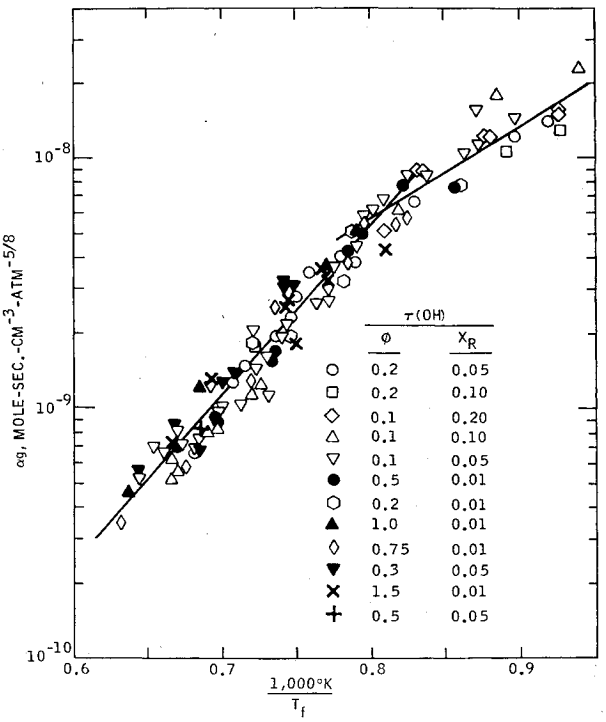

Fig. 5 Correlated reaction period data for τ(OH) in $C_3H_8 + O_2 + Ar$.

for all parameters and

$$g = X_R^{-0.8}\phi^{-0.7} \text{ for } \tau = \tau(\text{OH}), \tau(\text{CO}_2), \tau(\text{RIG}) \quad (1a)$$

$$g = X_R^{-0.2}\phi^{-n'};\ \ln n' = 0.6 - 45\,X_R \text{ for } \tau = \tau'_I(\text{OH}) \quad (1b)$$

$$g = X_R^{0.1}\phi^{-n};\ \ln n = 0.3 - 30\,X_R \text{ for } \tau = \tau_I(\text{OH}), \tau_I(\text{CO}_2) \quad (1c)$$

The factor 5 appearing in Eq. (1) is the oxygen to propane concentration ratio for a stoichiometric mixture. In terms of concentrations in mole-cm^{-3},

$$\alpha = (C_3H_8)^{1/2}(O_2)^{1/2}P_f^{-5/8}\tau \quad (2)$$

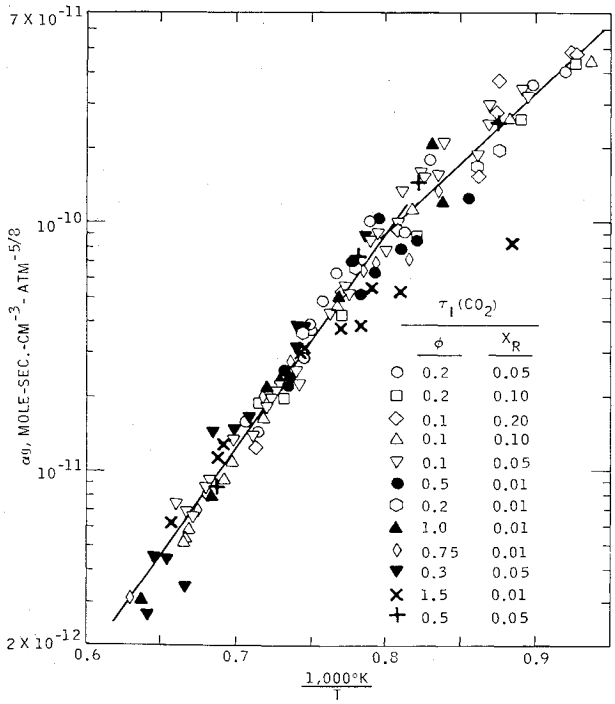

Fig. 6 Correlated induction period data for $\tau_I(CO_2)$ in $C_3H_8 + O_2 + Ar$.

where the concentrations are computed using P_f and T_f. Note that the factor $(C_3H_8)^m(O_2)^{1-m}\tau$, where $0 \leq m \leq 1$ and τ is the characteristic time, has been used previously[17] to successfully correlate induction period data for C_2H_2 and C_2H_4 oxidation. The calculation of τ from the laboratory times and the use of P_f and T_f in the correlations are discussed below. The major differences in αg for the ignition delay and the reaction times are that 1) the dependence of ignition delay on ϕ changes with X_R whereas the reaction time dependence on ϕ does not and 2) the ignition delay time is more strongly dependent on X_R than is the reaction time. For the ignition delay data, at $X_R = 0.20$, $g \sim 1$ to a good approximation. The straight lines drawn through the data in Figs. 5 and 6 are the least squares fit to the data for the temperature intervals above and below 1250°K. These curves demonstrate the difference in the temperature dependence of all the parameters above and below about 1250°K as noted previously. Also, the reaction and ignition delay parameters for $X_R = 0.01$ and $\phi = 1.5$ show large deviations from the fits which increase with decreasing temperature at temperatures below 1300°K; this is obvious in Fig. 6. The fits for all the parameters, based on 133 experiments, are given in Table 2 in the form

$$\alpha g = C_0(\tau)\exp[E_a(\tau)/RT_f] \quad (3)$$

The curves for the various parameters normalized according to Eqs. (1–1c) are compared in Fig. 7, where the error bars represent the standard deviations for the data. The curves for $\tau(CO_2)$, τ(OH), and τ(RIG) and for τ_I(OH) and $\tau_I(CO_2)$ are not significantly different. By contrast, the curve for τ'_I(OH) is significantly different from the τ_I curves. [But observe that a comparison of the curves representing τ_I and τ'_I(OH) depends on X_R and ϕ in addition to the ratio τ_I/τ'_I(OH).] The agreement of the curves for the reaction time parameters as well as of the curves for two of the ignition delay parameters strongly depends on the sensitivities of the detection system toward the emission of OH and CO_2 and the changes in refractive index gradient. In the present study, changes of roughly 0.04 mole % CO_2, $\lesssim 10^{-3}$ mole % OH, and a gradient of 10^{-6}-g-liter^{-1}-mm^{-1} could be detected. As a consequence of this dependence upon the detector sensitivity, no significance can be attributed to the observed agreement in terms of chemical kinetics. Furthermore, the arbitrary nature of any experimental definition of reaction time (and also of ignition delay time) is evident from these considerations.

Summary and Discussion

Empirical correlations between reaction and ignition delay times and the temperature, pressure, and equivalence ratio

Table 2 Least square fits to correlated data

Parameter	T, °K	C_0	E_a, kcal/mole	D^a
τ_I'(OH)	>1250	0.535×10^{-19}	51.3	26.0
τ_I(OH)	<1250	0.257×10^{-14}	26.0	17.6
	>1250	0.188×10^{-17}	44.3	12.8
$\tau_I(CO_2)$	<1250	0.255×10^{-14}	26.0	18.9
	>1250	0.884×10^{-17}	40.2	14.0
τ(OH)	<1250	0.634×10^{-11}	17.0	18.1
	>1250	0.189×10^{-13}	31.3	15.8
$\tau(CO_2)$	<1250	0.127×10^{-10}	15.4	20.7
	>1250	0.271×10^{-13}	30.9	14.4
τ(RIG)	<1250	0.186×10^{-10}	14.6	18.6
	>1250	0.582×10^{-14}	35.0	22.2

[a] % deviation $= \dfrac{100\Sigma\{|(\alpha g) - (\alpha g)_{\text{calc}}|\}/(\alpha g)_{\text{calc}}}{N}$; N = number of experiments.

have been obtained in the following forms:

$$\tau = \frac{C_0(\tau)R'T_f}{P_f^{3/8}X_R^{0.2}}\frac{\phi^{0.2}(5+\phi)}{(5)^{1/2}}\exp[E_a(\tau)/RT_f] \quad (4a)$$

$$\tau'_I = \frac{C_0(\tau'_I)R'T_f}{P_f^{3/8}X_R^{1.2}}\frac{\phi^{n'-1/2}(5+\phi)}{(5)^{1/2}}\exp[E_a(\tau'_I)/RT_f];$$

$$\ln n' = 0.6 - 45\,X_R \quad (4b)$$

$$\tau_I = \frac{C_0(\tau_I)R'T_f}{P_f^{3/8}X_R^{1.1}}\frac{\phi^{n-1/2}(5+\phi)}{(5)^{1/2}}\exp[E_a(\tau_I)/RT_f];$$

$$\ln n = 0.3 - 30\,X_R \quad (4c)$$

for experiments on the oxidation of propane where $1000°K < T < 1600°K$, $0.5\text{ atm} < P < 5.5\text{ atm}$, $0.01 \leq X_R \leq 0.20$, and $0.1 \leq \phi \leq 1.5$. Equation (4b) is to be used only for $T > 1250°K$. Note that the occurrence of detonations limited the accessible combinations of pressure, temperature, and composition within these ranges; *thus, the empirical correlations are based on a restricted coverage of these ranges.* (For a complete listing of the experimental conditions and of the reaction and ignition delay times, see Table 3 of Ref. 14.) The values of $C_0(\tau)$ and $E_a(\tau)$ are listed in Table 2.

A major problem in establishing meaningful correlations is the conversion of the ignition delay and reaction times from the laboratory to the particle coordinate system. Four factors enter into this conversion. First, shock wave attenuation results in an increase in the temperature as a function of distance behind the shock front.[18] Second, the boundary-layer growth results in an increase of the density as a function of distance behind the shock front and also a significant increase in the flight time of a particle, in shock-fixed coordinates, to points between the shock front and the contact surface.[19,20] Third, flow instabilities introduce uncertainties in the time progress of reactions. Fourth, even in an ideal flow, the coupling between the changing temperature, pressure, and the progress of the chemical reactions is difficult to take into account. In the ideal flow case, problems connected with the fourth factor can be avoided by comparing numerically computed time profiles of the observables with the experimental time profiles and altering the input to the numerical calculations until agreement between the calculations and experiments is reached. However, this requires a knowledge of the reaction mechanism which is lacking in the case of propane oxidation.

For the present experiments, the first factor, shock wave attenuation, results in a maximum temperature increase of less than 1.4% for $T > 1250°K$ and less than 2.8% for $T > 1430°K$. No correction for this has been made to the data.

The effect of the second factor, boundary-layer growth, is difficult to assess because the necessary theoretical analysis has been developed[19] strictly only for the case where the limiting separation between the shock front and contact surface l_m has been reached for low-pressure shock tube operation. In the propane oxidation experiments, the limiting separation l_m has not been reached by the time the shock wave passes the observation station and the initial pressures used are relatively high (for all experiments $P_1 \geq 22$ mm Hg and for 69% of all experiments, $P_1 \geq 45$ mm Hg). However, the increase in particle residence time, resulting from mass flow into the boundary layer, is estimated to be less than 2% for the propane oxidation experiments. These estimates are based on the observation[20] that the theoretical formula[19,20] for correcting the particle flight time is adequate for experimental use when the limiting separation is not reached and on the assumption that the estimates are conservative when applied to data obtained with relatively large initial test gas pressures. If the time of flight correction were significant, then the characteristic times at lower temperatures would be increased by larger factors than those times measured at higher temperatures. The effect of such a correction would be to reduce or perhaps eliminate the distinct changes in slope

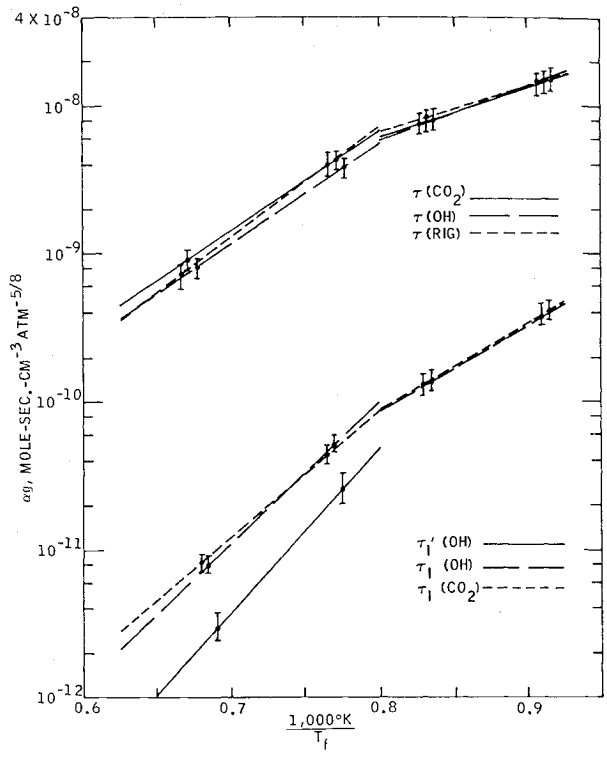

Fig. 7 Least square fits for reaction and ignition delay parameters.

at approximately 1250°K which occurs, for example, in Figs. 5 and 6. However, this apparently is not the case with the present experiments; alternatively the change in slope may result from a change in the mechanism of oxidation when the experimental temperature is increased beyond 1250°K. Evidence for this possibility has been obtained in the oxidation of methane[21] behind reflected shock waves. Here, the reacting gas mixture is essentially quiescent and the preceding correction is not applicable.

In addition to the increased particle residence time, the boundary-layer growth results in a temperature increase, which, for the propane oxidation experiments, is estimated to be less than 1%; this estimate is based on the assumption that the analysis developed[19] for the case of limiting separation and low-pressure experiments can be applied to the propane oxidation data. No corrections to the latter data for the effects of boundary-layer growth considered here have been made.

The third factor, flow instabilities, may also produce systematic errors in the data interpretation. Because flow instabilities are more likely to occur when shorter characteristic times are measured, the data obtained at higher temperature are probably more influenced. However, the actual magnitude of the effect of flow instabilities on the characteristic times is unknown. In fact, the temperature dependence is the same for data obtained with unstable flows (as determined on the basis of the experimental flow instability criteria developed in this study) and those obtained with apparently stable flows. (All of the data used to establish the correlations were obtained in experiments for which the shock wave velocity was observed only to attenuate.) Also, the scatter in the data is not large for shock tube experiments. These facts indicate that the experiments with flow instabilities yielded data which were not significantly different from data obtained in the absence of detectable flow instabilities.

The fourth factor was evaluated using the following approximate procedure. The refractive index gradient extrema were determined from the recorded profile and each location was considered as corresponding to a density jump $\Delta\rho_i$ given by the relation $\Delta\rho_i = (A_i/\Sigma_i A_i)(\rho_e - \rho_f)$. The result was

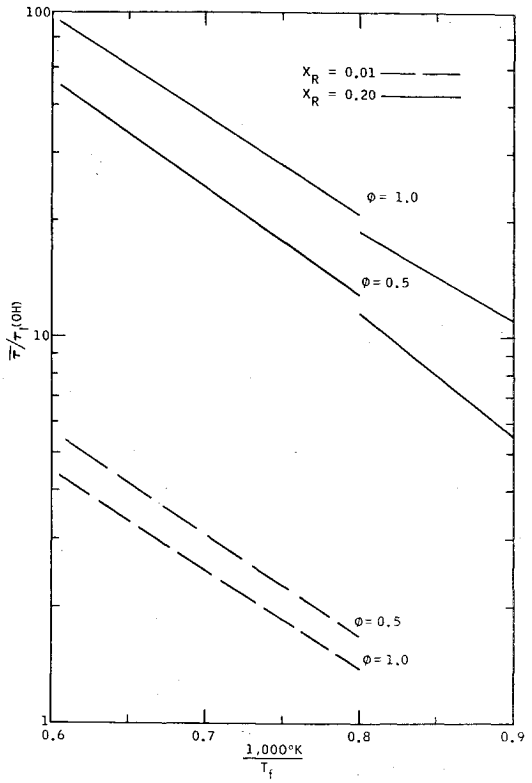

Fig. 8 Ratio of reaction time to ignition delay time $C_3H_8 + O_2 + Ar$.

the construction of a density profile which appeared as a set of steps. In calculating the densities for various steps, the assumptions of constant pressure and molecular weight of the gas mixture for the total reaction time were made. From the density profile, the corrected reaction times were computed. The application of this procedure resulted in a change in τ of less than -20% for all the runs and in a change of only -10% or less for about 90% of the runs. This was found provided the temperature of the experiment was regarded to be T_f. A time averaged value of the temperature computed from the density step profile could have been used in the correlation, but it is not more meaningful and introduces a dependence on the density step model into the correlations. In view of the small changes in τ from the application of the foregoing procedure to the data, the correlations were established using characteristic times computed from $\tau_p = (\rho_{fl})\tau_L$.

In spite of the reservations with which the correlations must be considered, two consequences of these relations are worthy of elaboration. First, the ratio of the reaction to ignition delay time $\bar{\tau}/\tau_I$ is significantly greater than one and for the case of most interest in SCRAMJET applications, i.e., with $X_R = 0.20$, this ratio is greater than 10 and becomes of the order of 50 for certain cases. The ratio $\bar{\tau}/\tau_I$ is shown in Fig. 8 as a function of T_f^{-1}. Note that if τ'_I had been used in place of τ_I to compute this ratio, the values calculated would have been larger. (The discontinuities in Fig. 8, as well as Fig. 9, result primarily from the averaging processes mentioned below.) These curves were computed with the data of Table 2 and the following equation:

$$\frac{\bar{\tau}}{\tau_I} = \frac{C_0(\tau)}{C_0(\tau_I)} X_R^{0.9} \phi^{0.7-n} \exp\left[\frac{E_a(\tau) - E_a(\tau_I)}{RT_f}\right] \quad (5)$$

using $C_0[\tau(\mathrm{Av})]$ and $E_a[\tau(\mathrm{Av})]$ where $C_0[\tau(\mathrm{Av})]$ and $E_a[\tau(\mathrm{Av})]$ are the average values of C_0 and E_a. This equation clearly shows that the ratio $\bar{\tau}/\tau_I$ is independent of pressure P_f. Second, the pressure normalized reaction times $P_f^{3/8}\bar{\tau}$ are relatively insensitive to variations in ϕ and X_R but are strongly dependent on variations in temperature. This is illustrated in Fig. 9 using the values of $C_0[\tau(\mathrm{Av})]$ and $E_a[\tau(\mathrm{Av})]$ and Eq. (4a) suitably rearranged, for calculation.

Two general features of the mechanism of hydrocarbon oxidation are indicated by comparing the present results with independent studies. First, the largest increase in OH emission occurs during the time of heat release in the combustion and is therefore not associated with the ignition delay or induction period as in the case of hydrogen oxidation. This is supported by the time profiles of the observables in propane oxidation and also by studies on the oxidation of acetylene in shock waves.[22] Second, the structural features of the OH emission profile may be observed in the oxidation of the paraffin hydrocarbons, generally. This is supported by the OH emission profiles obtained in four different experiments[14,15,23] involving CH_4, C_3H_8, and C_8H_{18} with Ar or N_2 diluent and behind incident and reflected shock waves. Yet, in all cases, the OH emission-time profiles have an initial and second rise, two sharp maxima or evidence thereof, and a final broad maximum. The display of these structural features in the reflected shock experiments indicates that they are relatively independent of the effects of shock wave attenuation, boundary-layer growth (as this affects the incident shock wave), and difficulties resulting from reacting gas flow. The observation of common features in the OH emission-time history for a range of gas mixture compositions and experimental conditions points to common, mechanistic features in hydrocarbon oxidation. Thus, this observation is possibly in support of the hypothesis[5] that the combustion of (paraffin) hydrocarbons of greater molecular weight than propane can be represented instead by the combustion of the same mass of propane to obtain reaction and ignition delay times with sufficient accuracy for engineering purposes.

The comparison of the present experimental determination of reaction time with a recent attempt[5] to calculate the reaction time in propane oxidation as well as with earlier measurements[6] of reaction time in other systems, is instructive. Values of the ratio of the measured to the calculated[5] reaction time in propane oxidation decrease from about 6 at 1100°K to 1 at 1500°K. Thus the calculations predict a smaller reaction time generally and a smaller temperature coefficient for the reaction time. However, for the calculations, the reaction

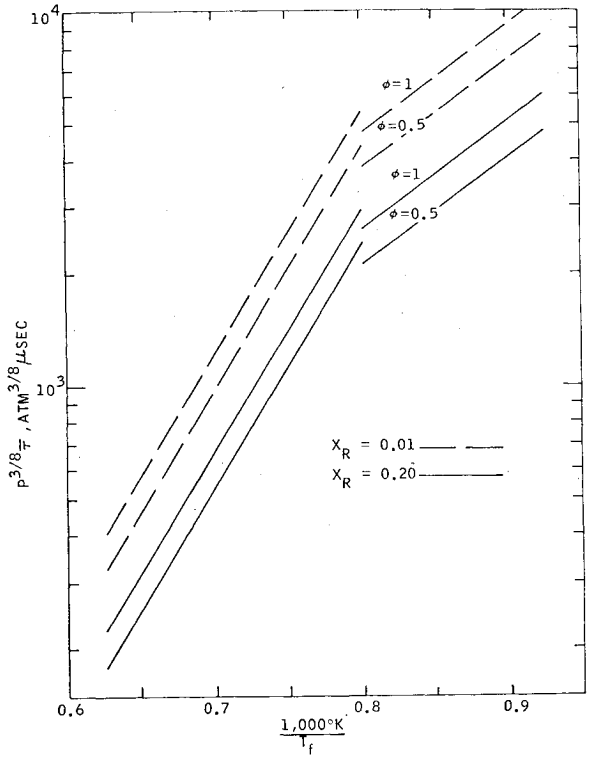

Fig. 9 Reaction times for $C_3H_8 + O_2 + Ar$.

time was defined as the time at which the temperature is equal to 95% of the final, equilibrium temperature. Since this definition differs from that used in the present experiments, the validity of comparing the calculations with the experimental results may be questioned.

A comparison of the ratios of the reaction time to the ignition delay time perhaps is less objectionable. In the present study, this ratio varied from 11 at 1100°K to 50 at 1550°K while the calculated ratios varied from about 2 to 5 in the same temperature interval for propane oxidation. For ethane oxidation, the calculated ratios varied from 2 to 30. The calculations and experiments agree in demonstrating an increase in the ratio of reaction to ignition delay time with increasing temperature, but the calculations predict smaller values for the ratio. Note that the calculations were performed for a system with N_2 as diluent but otherwise with the same parameters as the system to which the experimentally derived ratios apply.

In the propane oxidation experiments, the temperature and pressure dependence of the reaction and ignition delay times are found to be similar. This similarity has also been noted[6] in the case of kerosene and isooctane oxidation.

Previous studies of the ignition delay times in propane oxidation have been carried out experimentally[7,24] and numerically.[5] The present experimental data are in qualitative agreement with the results of these studies with respect to the inverse dependence of the ignition delay time on pressure, temperature, and the concentrations of fuel, oxygen, and diluent. The empirical correlations [Eqs. (4b) and (4c)] indicate an increase in ignition delay time with increasing ϕ as observed in other shock tube investigations[7] of propane oxidation at dilutions of 99% Ar and a decrease in ignition delay time with increasing ϕ as calculated[5] for propane oxidation at the smaller dilution of 80% N_2.

A quantitative comparison of the present experimental data with results of the previous[7] shock tube study of the ignition delay in propane oxidation is made difficult by the differences in 1) the method of defining the ignition delay time and 2) the spectral interval employed for observing emitted radiation and by the possible differences in sensitivity to the radiating species. However, the ignition delay times measured in the present experiments are the same, within an error less than ±25%, as those previously measured[7] at identical values of P, ϕ, and X_R and for comparable temperatures. For other values of the parameters, the previous investigators[7] observed a greater dependence of the ignition delay time on ϕ at dilutions of 95% Ar than the present correlations yield and did not distinguish two regimes for the temperature dependence as in the present report. With regard to the latter distinction, note that the present study involved a larger temperature range and that in the regime of temperatures below about 1250°K, the temperature coefficient found here is consistent with the temperature coefficient measured for propane oxidation between 800° and 1000°K in a flow apparatus.[24] At the highest common temperatures employed in the two shock tube investigations, the temperature coefficients tend to a similar value. In comparison with the calculated values[5] of the ignition delay time, the present experimental values are generally smaller by more than an order of magnitude except at temperatures below 1250°K.

References

[1] Ferri, A., "Review of Problems in Application of Supersonic Combustion," *Journal of the Royal Aeronautical Society*, Vol. 68, No. 645, Sept. 1964, pp. 575–597.

[2] Stull, F. D., "Scramjet Combustion Prospects," *Astronautics & Aeronautics*, Vol. 3, No. 12, Dec. 1965, pp. 48–52.

[3] Pergament, H. S., "A Theoretical Analysis of Nonequilibrium Hydrogen-Air Reactions in Flow Systems," AIAA Paper 63-113, White Oak, Md., 1963.

[4] Pergament, H. S., *Ninth Symposium (International) on Combustion*, Academic Press, New York, 1963, pp. 238–239.

[5] Chinitz, W. et al., "Analytical and Experimental Investigation of the Low Speed Fixed Geometry Supersonic Combustion Ramjet, Vol. I—Basic Technology Report," AFAPL-TR-66-102, Jan. 1967, General Applied Science Labs., Inc., Westbury, N.Y.

[6] Brokaw, R. S., "Thermal Ignition With Particular Reference to High Temperature," *Selected Combustion Problems*, Vol. 2, Butterworths, London, 1956, pp. 115–138.

[7] Hawthorn, R. D. and Nixon, A. C., "Shock Tube Ignition Delay Studies of Endothermic Fuels," *AIAA Journal*, Vol. 4, No. 3, March 1966, pp. 513–520.

[8] Sulzmann, K. G. P., "High Temperature, Shock Tube CO_2-Transmission Measurements at 4.25μ," *Journal of Quantitative Spectroscopy and Radiative Transfer*, Vol. 4, No. 3, May 1964, pp. 375–413.

[9] Myers, B. F. and Bartle, E. R., "I. Preparation of Test Gas Mixtures Containing Ozone, II. A Quick Change, High Vacuum Window, and Heat-Transfer Gauge Installation for Shock Tubes, III. A High Sensitivity, Low Cost, Electronic Integrator," TN GDC-DBE-66-008, July 1966, General Dynamics/Convair, San Diego, Calif.

[10] Ferriso, C. C. and Ludwig, C. B., "High-Temperature Spectral Emissivities of H_2O–CO_2 Mixtures in the 2:7-μ Region," *Applied Optics*, Vol. 3, No. 12, Dec. 1964, pp. 1435–1443.

[11] Myers, B. F. and Bartle, E. R., "Shock-Tube Study of the Radiative Processes in Systems Containing Atomic Oxygen and Carbon Monoxide at High Temperature," *Journal of Chemical Physics*, Vol. 47, No. 5, Sept. 1967, pp. 1783–1792.

[12] Myers, B. F. and Bartle, E. R., "A Shock-Tube Study of the Radiative Combination of Oxygen Atoms by Inverse Predissociation," *Journal of Chemical Physics*, Vol. 48, No. 9, May 1968, pp. 3935–3944.

[13] Kiefer, J. H. and Lutz, R. W., "Vibrational Relaxation of Deuterium by a Quantitative Schlieren Method," *Journal of Chemical Physics*, Vol. 44, No. 2, Jan. 1966, pp. 658–667.

[14] Myers, B. F. and Bartle, E. R., "Reaction Times of Hydrocarbon Oxidation Behind Incident Shock Waves in a Shock Tube," TR AFAPL-TR-152, Jan. 1968, General Dynamics/Convair, San Diego, Calif.

[15] Myers, B. F. and Bartle, E. R., "Reaction Times of Hydrocarbon Oxidation Behind Incident Shock Waves in a Shock Tube," Technical Performance Status Report, Contract F33615-67-C-1382, April 1967, General Dynamics/Convair, San Diego, Calif.

[16] Homer, J. B. and Kistiakowsky, G. B., "Acetylene-Oxygen Reaction in Shock Waves. Origin of CO_2," *Journal of Chemical Physics*, Vol. 46, No. 11, June 1967, pp. 4213–4218.

[17] White, D. R., "Density Induction Times in Very Lean Mixtures in D_2, H_2, C_2H_2 and C_2H_4 with O_2," *Eleventh Symposium (International) on Combustion*, The Combustion Institute, Pittsburgh, Pa., 1967, pp. 147–154.

[18] Strehlow, R. A., "Detonations and the Hydrodynamics of Reactive Shock Waves," 154th National American Chemical Society Meeting, *Symposium on Detonations and Reactions in Shock Waves*, American Chemical Society, Division of Fuel Chemistry, Preprint, Vol. 11, No. 4, Sept. 1967, pp. 1–28.

[19] Mirels, H., "Flow Nonuniformity in Shock Tubes Operating at Maximum Test Times," *The Physics of Fluids*, Vol. 9, No. 10, Oct. 1966, pp. 1907–1912.

[20] Fox, J. N., McLaren, T. I., and Hobson, R. M., "Test Time and Particle Paths in Low-Pressure Shock Tubes," *The Physics of Fluids*, Vol. 9, No. 12, Dec. 1966, pp. 2345–2350.

[21] Asaba, T. et al., "A Shock Tube Study of Ignition of Methane-Oxygen Mixtures," *Ninth Symposium (International) on Combustion*, Academic Press, New York, 1963, pp. 193–200.

[22] Gardiner, W. C., Jr. et al., "Heat-Release Profiles in the High-Temperature Oxidation of Acetylene in Shock Waves," *Journal of Chemical Physics*, Vol. 44, No. 12, June 1966, pp. 4653–4654.

[23] Seery, D. J. and Bowman, C. T., "A Shock Tube Study of Methane Oxidation," 154th National American Chemical Society Meeting, *Symposium on Detonations and Reactions in Shock Waves*, American Chemical Society, Division of Fuel Chemistry, Preprint, Vol. 11, No. 4, Sept. 1967, pp. 82–95.

[24] Brokaw, R. S. and Jackson, J. L., "Effect of Temperature, Pressure, and Composition on Ignition Delays for Propane Flames," *Fifth Symposium (International) on Combustion*, Reinhold, New York, 1955, pp. 563–569.